CRITICAL BEAM LOSSES DURING COMMISSIONING AND INITIAL OPERATION OF THE LHC

G. Robert-Demolaize, R. Aßmann, C. Bracco, S. Redaelli, T. Weiler, CERN, Geneva, Switzerland

Abstract

Results of first simulations with all movable elements of the LHC collimation system [1] for various operation modes are discussed. Compared to previous results, the inclusion of all collimators in the tracking brought down the beam losses by a factor 10 in the ideal machine case, i.e. nominal optic settings for both 450 GeV and 7 TeV energy. The sensitivity of the system to free orbit oscillations following multiple scenarios is addressed. These results show that it is sufficient to use a limited number of beam loss monitors (BLMs) for the setup and optimization of the LHC Collimation System.

INTRODUCTION

The main purpose of the LHC collimation system is to provide efficient cleaning and protection from halo losses using a combination of collimators and absorbers. During LHC operation, proton losses must be monitored in order to avoid quenches of superconducting magnets. Studies on quench levels for slow, continuous proton losses [2] give the maximum allowed proton loss rates for the LHC as:

$$R_q^{inj} = 7 \times 10^8 \text{ protons m}^{-1} \text{ s}^{-1} \text{ (450 GeV)} \quad (1)$$

$$R_q^{low\beta} = 7.8 \times 10^6 \text{ protons m}^{-1} \text{ s}^{-1} \text{ (7 TeV)} \quad (2)$$

For the nominal LHC beam intensity of 3×10^{14} protons, losses must be controlled for 10^{-6} to 10^{-8} of the total beam population to avoid limitation in maximum beam intensity. Understanding the cleaning performance of the collimation system is therefore mandatory for safe commissioning and operation of the LHC.

To monitor and control the losses, about 3700 BLMs are installed in the LHC for the two beam lines. In the early stages of machine commissioning, the full set of BLM information is not required. Two types of critical BLMs can be distinguished for study and commissioning of the collimation system:

- BLMs located close to the collimators and absorbers: required for the beam-based alignment of the movable elements to get the correct opening of the collimator jaws [3],

- BLMs at critical loss locations of the leakage halo: the halo exiting the LHC cleaning insertions (momentum or betatron) gets lost in characteristic locations, hence determining the efficiency of the system.

Identifying the BLM channels needed for early operation requires the study of loss locations. This problem is addressed using state-of-the-art tracking tools which include a correct treatment of chromatic effects, non-linear fields and an aperture model with a 10 cm resolution [4]. For the first time, full simulations for the LHC have been performed taking into account all movable elements of the collimation system. This paper presents the results for beam halo tracking considering various ideal and error scenarios for Beam 1 and the betatron cleaning. A list of critical loss locations is introduced as a baseline for a minimum workable BLM system for commissionning and early operations of the LHC collimation system.

SCENARIOS FOR HALO TRACKING

The LHC collimators, located in the two warm insertions dedicated for cleaning, intercept beam halo. A small fraction of the halo leaks out and gets lost at characterisitc locations around the ring. The level of performance of the system is given by its *local cleaning inefficiency* η:

$$\eta = \frac{\text{number of protons lost in the machine aperture}}{\text{number of protons absorbed by the system} \times \text{L}}, \quad (3)$$

with *L* a given length of aperture, which will be 10 cm in the following. Critical loss locations are spotted by comparing the local inefficiency values with the magnet quench limits derived from (1), (2) (see Table 1 below) for estimated minimal beam lifetimes [5].

Simulations are first done for nominal machine optics. Afterwards error models are applied. The mechanical parameters of collimators are listed in Appendices A and B.

Nominal optics

The nominal reference cases are defined with the parameters listed in Tables 1 and 2.

Table 1: Optics parameters of the simulated nominal cases.

Case	E [TeV]	IR 1 & 5	IR 2 & 8
Injection	0.45	β^* = 17 m	β^* = 10 m
Collision	7	β^* = 0.55 m	β^* = 10 m

Table 2: Beam lifetimes τ and corresponding quench levels for the simulated nominal cases.

Case	τ [h]	$\tilde{\eta}_{quench}$ [m^{-1}]
Injection	0.1	10^{-3}
Collision	0.2	2×10^{-5}

Using this optics, one can generate horizontal and vertical halos and track them separately. The result is the loss map in the machine for the defined optics and energy. Description of the tracking tools can be found in [4].

Error scenario

In addition to the ideal case, a horizontal beam halo with a free closed orbit oscillation in the horizontal plane is considered. To take into account all possible cases for the error both in phases and amplitudes, two horizontal kickers were selected, separated by a phase advance of $\frac{\pi}{2}$ to allow a full phase scan within $[-\pi;\pi]$.

The worst phase is found by locating the most critical loss location, i.e. the 10 cm bin in which the most particles are lost. Once this phase is found, a scan in error amplitude for that phase is performed.

This whole process (phase + amplitude) is done for two different cases:

- static case: all collimators are recentered around the perturbed closed orbit and the amplitude of the error reaches the estimated tolerances of each operational mode: Table 3 summarize these tolerances values and Fig. 1 shows a sample perturbed orbit for the collision case,

- dynamic case: collimators are kept centered around the nominal closed orbit; the error amplitude can reach a maximum of about 1.5 σ.

Table 3: Closed orbit tolerances for the nominal optics.

Case	Arc tolerances	IR tolerances
Injection	$\pm$ 4 mm	$\pm$ 4 mm
Collision	$\pm$ 4 mm	$\pm$ 3 mm

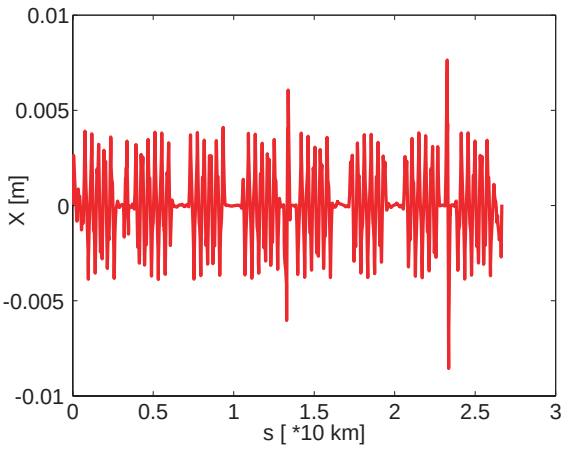

Figure 1: Horizontal closed orbit obtained for the static study in the collision case; the orbit was corrected in IR2, IR5 & IR8 to follow the nominal crossing schemes.

CRITICAL LOCATIONS FROM BEAM LOSS PATTERNS

Loss maps are obtained for the nominal and error scenarios described above. By comparing the ideal machine patterns with the perturbed cases, one can spot the critical loss locations in the superconducting regions of the machine.

Injection optics - Static scenario

A loss of a factor 2 in cleaning efficiency at the worst locations in the machine can be seen for the $\pm$ 4 mm horizontal orbit error case (Fig. 4). Detailed comparison of loss locations shows two important features:

- downstream of IR7, the loss locations are identical between the ideal and the perturbed case (see Fig. 2),

- the first loss locations downstream of IP7 correspond to the first two high dispersion locations, at the end of the dispersion suppressor (see Fig. 3).

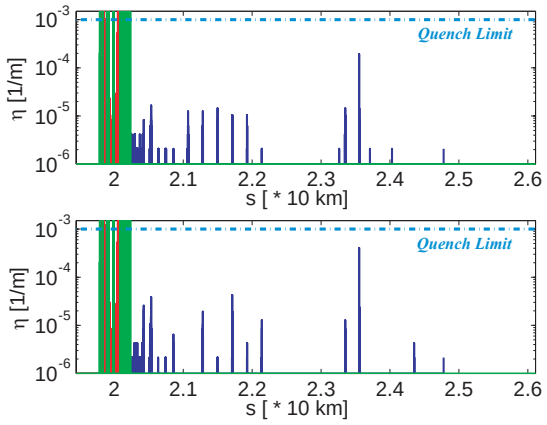

Figure 2: Beam loss patterns for injection from IR7 to the end of arc 8-1 for an ideal machine (top) and a $\pm$ 4 mm horizontal orbit perturbation (bottom).

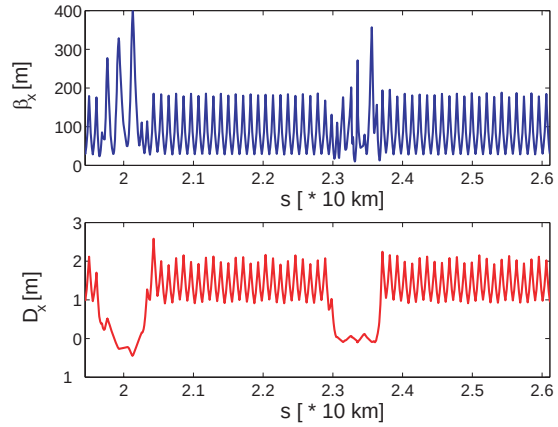

Figure 3: Optical function β_x (top) and dispersion function D_x (bottom) for injection from IR7 to the end of arc 8-1.

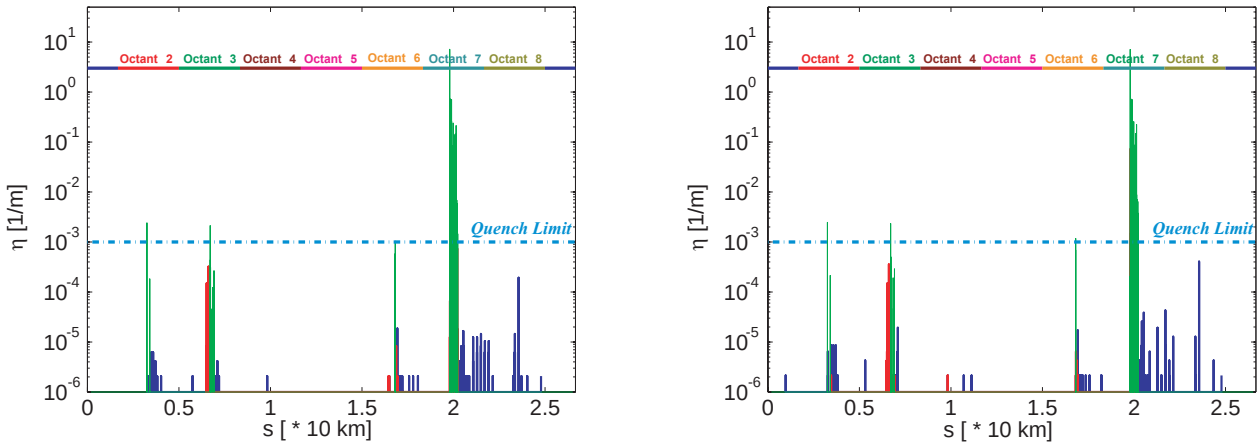

Figure 4: Global beam loss patterns for an ideal machine (top) and a 4 mm orbit offset (bottom) for injection.

Losses in the dispersion suppressor cannot be avoided: off-momentum halo is generated at the primary collimators due to single-diffractive scattering during the interaction between an incoming proton and the collimator material. The off-momentum protons will always get lost at the first high dispersion location. This defines a characteristic location for proton losses, but at the same time sets a fundamental limitation to the betatron cleaning efficiency.

Losses seen in the IR2 region come from particles being scattered off from the TDI jaws and then getting lost in the downstream cold aperture of the machine.

Going through the whole line (Beam 1), one can count 13 critical loss locations which should be added to the locations of the installed collimators. Additional locations must be identified around IR3 (momentum cleaning).

Collision optics - Static scenario

For collision (see Fig. 6, there are less loss locations along the machine compared to the injection optics case but at the same time a higher proportion of them are getting closer to the quench limit. When comparing the ideal machine case with the case of an orbit error reaching the tolerances in orbit offset, it can be seen in Fig. 6 that the cleaning system looses at a factor 2.98 in efficiency, with the losses in the dispersion suppressor going over the quench limit (instead of being just below it in the ideal case).

Going downstream of IR7 (see Fig. 5), it can be seen that the main loss locations are mostly identical for the ideal and the perturbed case; plus, if one would check the locations of the peaks showing up in the perturbed case, it can be noticed that they correspond to the critical locations already spotted in the injection case (with a few exceptions).

Additional locations for IR3 should be taken into account. Loss locations identified in our simulations only refer to protons getting directly lost in the cold aperture of the machine, but energy deposition studies are performed in parallel to check the influence of particle showers originated in the tertiary collimators (TCT) protecting the triplet magnets close to the experimental insertions.

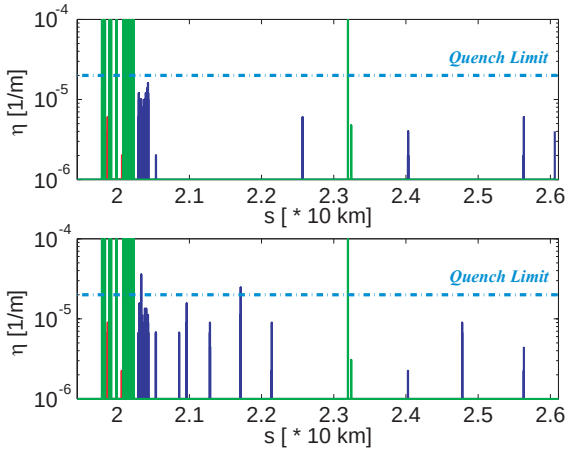

Figure 5: Beam loss patterns for collision from IR7 to the end of arc 8-1 for an ideal machine (top) and a 3 mm (IR)/4 mm (arc) orbit perturbation (bottom).

Counting losses from the halo exiting the betatron cleaning insertion, one finds 18 locations for critical BLMs at collision.

Summary

After having scanned all phases and amplitudes in the static scenario, it was possible to spot 13 critical locations for injection and 18 for collision. This sums up to 25 different locations though, as 6 elements are critical in both cases: these 6 locations correspond to the end of the dispersion suppressor of IR7 and the arc between insertions 7 and 8.

Tables 4 and 5 summarize the predicted locations for "golden" BLMs, i.e. characteristic loss locations due to the collimation system. These locations form the minimum workable LHC BLM system for the set-up and commissioning of the collimation system. BLMs at similar locations around IR3 and at the triplet magnets must be added.

The tracking tools also allow checking the longitudinal

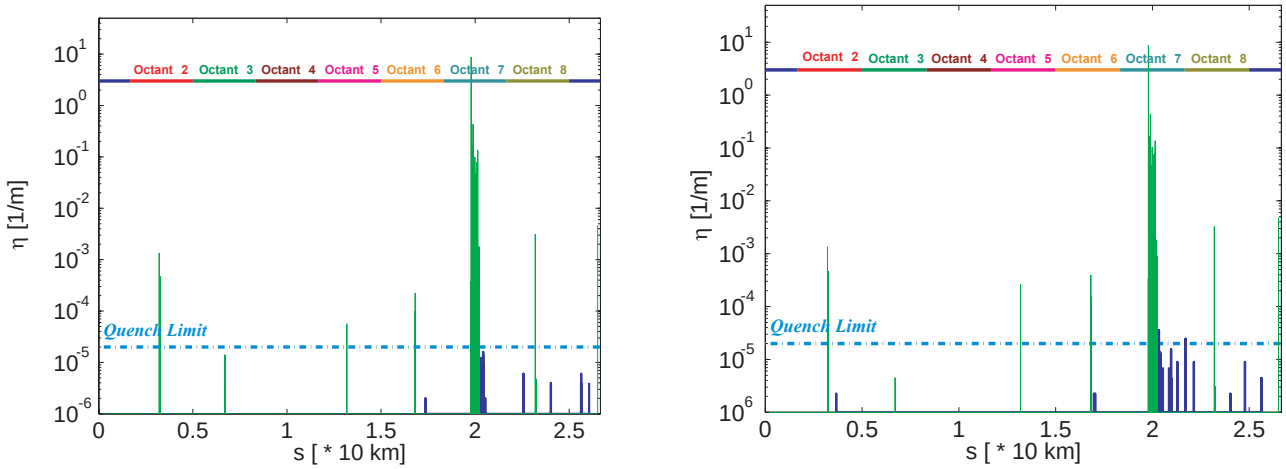

Figure 6: Global beam loss patterns for an ideal machine (top) and a 3 mm (IR)/4 mm (arc) orbit offset (bottom) for collision.

Table 4: Critical loss locations at injection optics.

Element	Location
Q11	right of IR3
DFBA @ Q5	right of IR6
Q11	right of IR7
Q13	right of IR7
Q23	right of IR7
Q27	right of IR7
Q31	right of IR7
Q33	left of IR8
Q29	left of IR8
Q25	left of IR8
Q2	right of IR8
Q6	right of IR8

Table 5: Critical loss locations at collision.

Element	Location
Q6	left of IR3
Q8	right of IR7
MB9	right of IR7
Q9	right of IR7
MB11	right of IR7
Q11	right of IR7
Q13	right of IR7
Q19	right of IR7
Q21	right of IR7
Q27	right of IR7
Q33	left of IR8
Q25	left of IR8
Q17	left of IR8
Q16	right of IR8
Q30	right of IR8
Q22	left of IR1
Q14	left of IR1

distribution of losses over any magnetic element. Fig. 7 shows an example of the longitudinal loss distribution. The planned geometry of the BLM system for each element is shown in Fig. 8. By comparing the two figures, we can see that it would be sufficient to use the channels from the first 2 BLMs at a quadrupole since the losses appear to be concentrated at the beginning of the element (see also [6] for more details).

PRELIMINARY RESULTS FOR THE DYNAMIC SCENARIO

The dynamic scenario is used to check of the sensitivity of the betatron cleaning system to orbit perturbations. In order to do so, it is assumed that the worst case occurs when a secondary collimator becomes a primary collimator due to an orbit error. The worst phase for the error would then leave the orbit unchanged at the primary collimator and create a maximum offset at a critical secondary collimator.

For a horizontal halo, the relevant horizontal primary collimator is the TCP.C6L7 and the critical horizontal secondary collimator is the TCSG.B4L7. The tracked orbits for a 0.4 σ (solid), 0.95 σ (dash-dotted) and 1.1 σ (dashed) offset are shown in Fig. 9. In the latter case, the secondary collimator becomes a primary. Tracking these orbits allows checking how much is lost in performance of the IR7 collimation system. This is done by comparing the values of the global inefficiency of the system at a given amplitude (e.g. the cold aperture of the machine) for

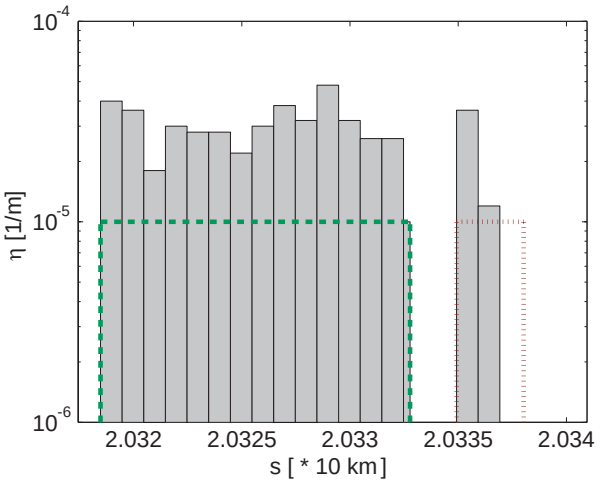

Figure 7: Beam loss pattern for a 1 m long bin for collision in the dispersion suppressor downstream of IP7: longitudinal distribution of the losses along a dipole magnet (dashed box) and a quadrupole magnet (dotted box).

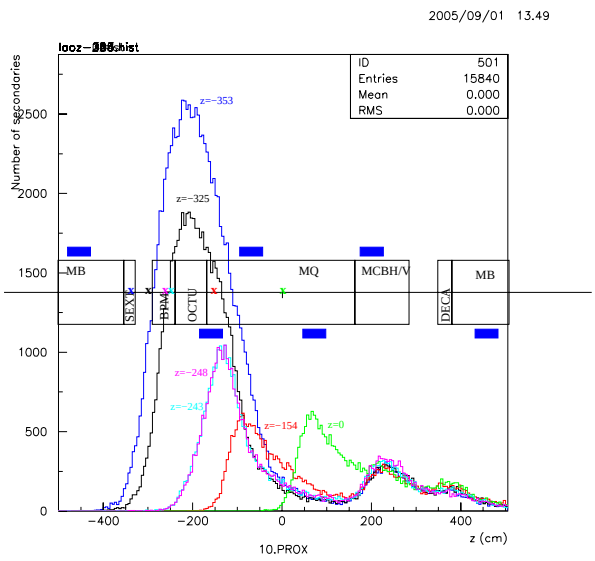

Figure 8: Shower development in the cryostat of a quadrupole. The positioning of the detectors (blue boxes) has been optimized to catch losses and to minimize uncertainty of ratio of energy deposition in coil and detector (courtesy of L. Ponce).

each orbit configuration. Results are shown in Fig. 10 for collision.

It is noted that the sextupoles were turned off in these simulations in order to keep the impact parameter at the collimator constant between the different cases. Fig. 10 shows that we loose a factor 8.68 in cleaning efficiency at collision if one of the secondary collimators becomes the primary collimator. Further studies on theses accident cases are currently being performed to analyze effects on beam loss patterns and BLM thresholds.

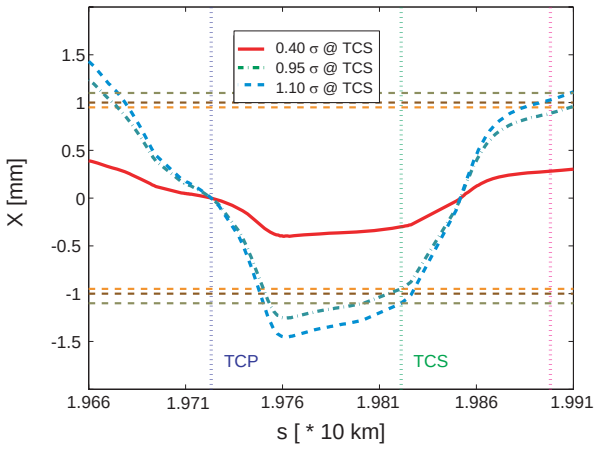

Figure 9: Orbit oscillations over 250 meters of the IR7 betatron cleaning insertion. The orbit at the horizontal primary collimator is left unchanged while 3 different offsets are applied at the relevant secondary collimator.

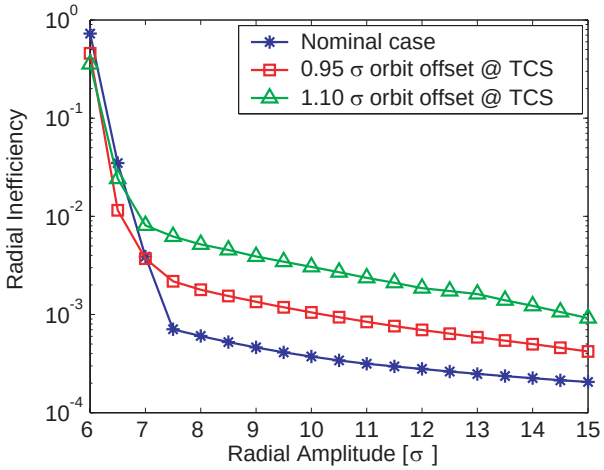

Figure 10: Global inefficiency curves at different orbit offset for the dynamic scenario. The system looses a factor 8.68 in efficiency when a secondary collimator becomes a primary.

CONCLUSION

The response of the LHC collimation system to free orbit oscillations for Beam 1 has been reviewed. With the specified LHC orbit errors, critical locations along the machine can be identified and used to define a minimum workable BLM system for the commissioning and set-up of the collimators during the early stages of operations. Some locations are critical for 450 GeV and 7 TeV. The dispersion suppressor immediately downstream of IP7 is the most critical region of the machine, with many losses concentrated over a few elements (the equivalent of two cells of the lattice). Energy deposition studies are ongoing for particle showers generated by inelastic proton-matter interaction in the tertiary collimators (close to the triplet magnets) and downstream of the beam dump protection equipment

(TCDQ). Additional locations should be obtained from simulations for the momentum cleaning insertion.

Further studies are planned to include beta-beating errors, tables of magnetic field errors for the dipoles, alignment errors for magnets in the aperture models and error scenarios for the mechanical parameters of the collimators (e.g. longitudinal tilt angle of one jaw). The setup for tracking of Beam 2 is also being finalized.

AKNOWLEDGEMENTS

The authors would like to thank T. Risselada and W. Herr from the AB/ABP group and J. Wenninger from the AB/OP group for the help provided on the generation of optics files. Many thanks also to B. Dehning, E. Holzer and L. Ponce from the AB/BDI group for discussions on the setup of the BLM system. Thanks to A. Bertarelli, M. Magistris and M. Santana-Leitner from the AB/ATB for their energy deposition studies with FLUKA. Finally, thanks to F. Schmidt and E. McIntosh for the support they provided on the development of the tracking code.

REFERENCES

[1] ”LHC Design Report”, Volume I, Ch. 18, CERN, 2004

[2] J.B. Jeanneret, D. Leroy, L. Oberli and T. Trenckler: ”Quench levels and transient beam losses in the LHC magnets”, CERN-LHC-PROJECT-REPORT-44, 1996.

[3] S. Redaelli: ”LHC aperture and commissioning of the collimation system”, Proc. Chamonix 2005.

[4] G. Robert-Demolaize, R. Aßmann, S. Redaelli, F. Schmidt: ”A new version of SixTrack with collimation and aperture interface”, Proc. PAC 2005.

[5] R. Aßmann: ”Collimators and cleaning: could this limit the LHC performance? ”, Proc. Chamonix 2003.

[6] B. Dehning: ”Commissioning of beam loss monitors”, these proceedings.

APPENDIX A

Table 6: Mechanical parameters of Phase 1 collimators for injection. Collimators which are not used at that energy are set to a 900 σ opening.

Name	Length [m]	Angle [radians]	Material	Halfgap [m]	Halfgap [σ]
TCL.5R1.B1	1.00	0.000	CU	1.242	900.0
TCTH.L2.B1	1.00	0.000	W	0.5477	900.0
TDI.4L2	4.00	1.571	CU	4.092×10^{-3}	6.8
TCTV.4L2.B1	1.00	1.571	W	0.5837	900.0
TCLIA.4R2.B1	1.00	1.571	C	6.531×10^{-3}	6.8
TCLIB.6R2	1.00	1.571	C	3.231×10^{-3}	6.8
TCP.6L3.B1	0.60	0.000	C	7.891×10^{-3}	8.0
TCSG.5L3.B1	1.00	0.000	C	5.913×10^{-3}	9.3
TCSG.4R3.B1	1.00	0.000	C	4.067×10^{-3}	9.3
TCSG.A5R3.B1	1.00	2.980	C	5.288×10^{-3}	9.3
TCSG.B5R3.B1	1.00	0.189	C	5.931×10^{-3}	9.3
TCLA.A5R3.B1	1.00	1.571	W	1.143×10^{-2}	10.0
TCLA.B5R3.B1	1.00	0.000	W	1.060×10^{-2}	10.0
TCLA.6R3.B1	1.00	0.000	W	9.759×10^{-3}	10.0
TCLA.7R3.B1	1.00	0.000	W	6.931×10^{-3}	10.0
TCTH.L5.B1	1.00	0.000	W	1.001	900.0
TCTV.L5.B1	1.00	1.571	W	0.744	900.0
TCL.5R5.B1	1.00	0.000	CU	1.254	900.0
TCDQ.4R6.B1	8.00	0.000	C	1.506×10^{-2}	8.0
TCS.TCDQ.B1	1.00	0.000	C	1.339×10^{-2}	7.0
TCP.D6L7.B1	0.60	1.571	C	4.170×10^{-3}	5.7
TCP.C6L7.B1	0.60	0.000	C	6.168×10^{-3}	5.7
TCP.B6L7.B1	0.60	2.225	C	5.045×10^{-3}	5.7
TCSG.A6L7.B1	1.00	2.463	C	6.046×10^{-3}	6.7
TCSG.B5L7.B1	1.00	2.504	C	7.081×10^{-3}	6.7
TCSG.A5L7.B1	1.00	0.710	C	7.229×10^{-3}	6.7
TCSG.D4L7.B1	1.00	1.571	C	4.781×10^{-3}	6.7
TCSG.B4L7.B1	1.00	0.000	C	6.565×10^{-3}	6.7
TCSG.A4L7.B1	1.00	2.349	C	6.664×10^{-3}	6.7
TCSG.A4R7.B1	1.00	0.808	C	6.708×10^{-3}	6.7
TCSG.B5R7.B1	1.00	2.470	C	7.797×10^{-3}	6.7
TCSG.D5R7.B1	1.00	0.897	C	7.809×10^{-3}	6.7
TCSG.E5R7.B1	1.00	2.277	C	7.828×10^{-3}	6.7
TCSG.6R7.B1	1.00	0.009	C	1.074×10^{-2}	6.7
TCLA.A6R7.B1	1.00	1.571	W	5.744×10^{-3}	10.0
TCLA.C6R7.B1	1.00	0.000	W	1.092×10^{-2}	10.0
TCLA.E6R7.B1	1.00	1.571	W	1.052×10^{-2}	10.0
TCLA.F6R7.B1	1.00	0.000	W	6.750×10^{-3}	10.0
TCLA.A7R7.B1	1.00	0.000	W	6.604×10^{-3}	10.0
TCTH.L8.B1	1.00	0.000	W	0.528	900.0
TCTV.4L8.B1	1.00	1.571	W	0.558	900.0
TCTH.L1.B1	1.00	0.000	W	1.001	900.0
TCTV.L1.B1	1.00	1.571	W	0.744	900.0

APPENDIX B

Table 7: Mechanical parameters of Phase 1 collimators for collision. Collimators which are not used at that energy are set to a 900 σ opening.

Name	Length [m]	Angle [radians]	Material	Halfgap [m]	Halfgap [σ]
TCL.5R1.B1	1.00	0.000	CU	2.575×10^{-3}	10.0
TCTH.L2.B1	1.00	0.000	W	1.327×10^{-3}	8.3
TDI.4L2	4.00	1.571	CU	0.142	900.0
TCTV.4L2.B1	1.00	1.571	W	1.414×10^{-3}	8.3
TCLIA.4R2.B1	1.00	1.571	C	0.227	900.0
TCLIB.6R2	1.00	1.571	C	0.112	900.0
TCP.6L3.B1	0.60	0.000	C	3.881×10^{-3}	15.0
TCSG.5L3.B1	1.00	0.000	C	2.999×10^{-3}	18.0
TCSG.4R3.B1	1.00	0.000	C	2.068×10^{-3}	18.0
TCSG.A5R3.B1	1.00	2.980	C	2.686×10^{-3}	18.0
TCSG.B5R3.B1	1.00	0.189	C	3.011×10^{-3}	18.0
TCLA.A5R3.B1	1.00	1.571	W	6.002×10^{-2}	20.0
TCLA.B5R3.B1	1.00	0.000	W	5.554×10^{-2}	20.0
TCLA.6R3.B1	1.00	0.000	W	5.115×10^{-3}	20.0
TCLA.7R3.B1	1.00	0.000	W	3.644×10^{-3}	20.0
TCTH.L5.B1	1.00	0.000	W	7.551×10^{-3}	8.3
TCTV.L5.B1	1.00	1.571	W	4.772×10^{-3}	8.3
TCL.5R5.B1	1.00	0.000	CU	2.543×10^{-3}	10.0
TCDQ.4R6.B1	8.00	0.000	C	3.951×10^{-3}	8.0
TCS.TCDQ.B1	1.00	0.000	C	3.764×10^{-3}	7.5
TCP.D6L7.B1	0.60	1.571	C	1.153×10^{-3}	6.0
TCP.C6L7.B1	0.60	0.000	C	1.703×10^{-3}	6.0
TCP.B6L7.B1	0.60	2.225	C	1.393×10^{-3}	6.0
TCSG.A6L7.B1	1.00	2.463	C	1.658×10^{-3}	7.0
TCSG.B5L7.B1	1.00	2.504	C	1.941×10^{-3}	7.0
TCSG.A5L7.B1	1.00	0.710	C	1.982×10^{-3}	7.0
TCSG.D4L7.B1	1.00	1.571	C	1.310×10^{-3}	7.0
TCSG.B4L7.B1	1.00	0.000	C	1.798×10^{-3}	7.0
TCSG.A4L7.B1	1.00	2.349	C	1.826×10^{-3}	7.0
TCSG.A4R7.B1	1.00	0.808	C	1.838×10^{-3}	7.0
TCSG.B5R7.B1	1.00	2.470	C	2.140×10^{-3}	7.0
TCSG.D5R7.B1	1.00	0.897	C	2.143×10^{-3}	7.0
TCSG.E5R7.B1	1.00	2.277	C	2.149×10^{-3}	7.0
TCSG.6R7.B1	1.00	0.009	C	2.949×10^{-3}	7.0
TCLA.A6R7.B1	1.00	1.571	W	1.509×10^{-3}	10.0
TCLA.C6R7.B1	1.00	0.000	W	2.870×10^{-2}	10.0
TCLA.E6R7.B1	1.00	1.571	W	2.759×10^{-2}	10.0
TCLA.F6R7.B1	1.00	0.000	W	1.774×10^{-3}	10.0
TCLA.A7R7.B1	1.00	0.000	W	1.734×10^{-3}	10.0
TCTH.L8.B1	1.00	0.000	W	1.277×10^{-3}	8.3
TCTV.4L8.B1	1.00	1.571	W	1.353×10^{-3}	8.3
TCTH.L1.B1	1.00	0.000	W	7.556×10^{-3}	8.3
TCTV.L1.B1	1.00	1.571	W	4.776×10^{-3}	8.3